International Journal of Bifurcation and Chaos, Vol. 19, No. 12 (2009) 4097–4106

EXISTENCE OF LIMIT CYCLES IN THE REPRESSILATOR EQUATIONS

OLGUŢA BUŞE, ALEXEY KUZNETSOV* and RODRIGO A. PÉREZ
Department of Mathematical Sciences, IUPUI,
**Center for Mathematical Biosciences, IUPUI,*
402 N. Blackford St., Indianapolis, IN 46202, USA

Received April 10, 2008; Revised May 4, 2009

The Repressilator is a genetic regulatory network used to model oscillatory behavior of more complex regulatory networks like the circadian clock. We prove that the Repressilator equations undergo a supercritical Hopf bifurcation as the maximal rate of protein synthesis increases, and find a large range of parameters for which there is a cycle.

Keywords: Limit cycles; oscillatory regulatory networks; repressilator.

1. Introduction

Regulatory networks are collections of interacting molecules in a cell. One particular kind, oscillatory networks, has been discovered in many biological processes. Well-known examples are the circadian clock [Dunlap, 1999] and the cell cycle [Nurse, 2000], where the oscillatory nature of the process plays a central role.

In recent years, researchers have been able to implement artificial regulatory networks in the laboratory. Studying these simplified models is an important step to understand real life networks.

Modeling studies suggest several designs for artificial oscillatory networks. There are many implementations of hysteresis-based oscillators, [Atkinson *et al.*, 2003; Barkai & Leibler, 2000; Hasty *et al.*, 2001; Kuznetsov *et al.*, 2004].

Another artificial oscillatory network called the Repressilator [Elowitz & Leiber, 2000] borrows the idea of a ring oscillator from engineering. The mechanism is based on connecting an odd number of inverters (negative control elements) in a ring. Its genetic implementation uses three proteins that cyclically repress the synthesis of one another. Our computational study [Yang *et al.*, 2009] suggests that the oscillatory mechanism of the repressilator is qualitatively different from that in other genetic oscillators. Moreover, the mathematical analysis of such a system has not been done. In this paper, we study the behavior of the following parametric family of differential equations:

Definition 1. Fix $n > 0$. For $\alpha > 0$ the Repressilator equations are

$$\begin{aligned} \frac{\mathrm{d}x}{\mathrm{d}t} &= \frac{\alpha}{1+y^n} - x \\ \frac{\mathrm{d}y}{\mathrm{d}t} &= \frac{\alpha}{1+z^n} - y \\ \frac{\mathrm{d}z}{\mathrm{d}t} &= \frac{\alpha}{1+x^n} - z \quad (x, y, z \geq 0). \end{aligned} \tag{1}$$

This is a reduced version of the original model in which three of six equations are assumed to be in quasi-equilibrium and substituted by algebraic relations. The reduction assumes that the three excluded variables evolve an order of magnitude faster than the other three. Note that when any of the three variables is 0, the corresponding derivative

is positive, so the orbit of any initial point with nonnegative coordinates moves in the positive octant $\{x, y, z > 0\}$ and remains there for all $t > 0$.

Our analysis is split in two parts. First, we describe the bifurcation behavior of the family. It is not hard to see that there is a unique fixed point R, which sits on the main diagonal.

Proposition 1. *The linearization of system (1) at R has one negative eigenvalue and a pair of complex conjugate eigenvalues.*

(a) *If $n \leq 2$ the complex eigenvalues have negative real part, so R is always attracting.*
(b) *If $n > 2$ there is a single supercritical Hopf bifurcation when $\alpha = \alpha_{\text{bif}} = r_0^{n+1} + r_0$, where $r_0 = \sqrt[n]{2/(n-2)}$.*

In the second part of the paper, we study the topological behavior of orbits. We begin by showing that in all cases the interesting behavior is restricted to a bounded region.

Lemma 1. *The orbit of any point P with nonnegative coordinates will eventually enter the cube $\mathcal{C} = \{0 \leq x, y, z \leq \alpha\}$ and stay in the interior of $\mathcal{C}$ thereafter.*

The fixed point R is always inside $\mathcal{C}$. When $n > 2$ and $\alpha > \alpha_{\text{bif}}$, R is a saddle, so standard index theory implies the existence of one or more attracting sets to "absorb" the orbits repelled by R.

Note that Proposition 1 already guarantees an attracting cycle near R when $0 < \alpha - \alpha_{\text{bif}} \ll 1$, because the bifurcation is supercritical. In fact there is always a cycle:

Theorem 1. *For $n > 2$ and all $\alpha > \alpha_{\text{bif}}$, system (1) has a limit cycle.*

Our proof is quasi-constructive and it yields more about the behavior of the orbits inside $\mathcal{C}$. We will describe a toroidal region $T \in \mathcal{C}$ that is partitioned into a chain of simply connected pieces, and show that the orbit of any point $P \in T$ travels in these six regions in a specific order. This proves the existence of a Poincaré map $\theta : K \to K$ where K is a section of T by a nullcline. Theorem (1) then follows from Brower's Fixed Point Theorem [Munkres, 2000, p. 351].

One advantage of our method is that the construction gives a heuristic reason for the existence of the cycle. This mechanism is qualitatively different from classical systems like the relaxation oscillator. An exploration of distinguishing features will appear in [Buşe *et al.*, 2009].

This paper is organized as follows: In Sec. 2 we prove Proposition 1 after describing the linearization of system (1) at R. The computation showing that the Hopf bifurcation is supercritical is delayed to an appendix at the end of the paper. In Sec. 3, we prove Lemma 1 and give a decomposition of $\mathcal{C}$ into pieces on which orbit behavior is simple to describe. Section 4 uses this decomposition to prove Theorem 1.

2. Bifurcation Analysis

From the description of nullclines in Sec. 3, it will follow that there is a unique equilibrium point R. Because of the symmetry between coordinates, R is of the form (r, r, r), where r satisfies

$$\frac{\alpha}{1 + r^n} = r; \tag{2}$$

i.e. $r^{n+1} + r - \alpha = 0$. This section is devoted to the analysis of the linearization of system (1) near R, which yields the proof of Proposition 1.

The jacobian matrix of (1) is:

$$J = \begin{pmatrix} -1 & \dfrac{-n\alpha y^{n-1}}{(1+y^n)^2} & 0 \\ 0 & -1 & \dfrac{-n\alpha z^{n-1}}{(1+z^n)^2} \\ \dfrac{-n\alpha x^{n-1}}{(1+x^n)^2} & 0 & -1 \end{pmatrix}, \tag{3}$$

so using (2), the linearization of system (1) at R is

$$\begin{pmatrix} \dfrac{\mathrm{d}u}{\mathrm{d}t} \\ \dfrac{\mathrm{d}v}{\mathrm{d}t} \\ \dfrac{\mathrm{d}w}{\mathrm{d}t} \end{pmatrix} = \begin{pmatrix} -1 & \dfrac{-nr^n}{1+r^n} & 0 \\ 0 & -1 & \dfrac{-nr^n}{1+r^n} \\ \dfrac{-nr^n}{1+r^n} & 0 & -1 \end{pmatrix} \cdot \begin{pmatrix} u \\ v \\ w \end{pmatrix}. \tag{4}$$

The eigenvalues of (4) are

$$\lambda = \omega \frac{nr^n}{1+r^n} - 1, \quad (\omega^3 = -1). \tag{5}$$

The eigenvalue corresponding to $\omega = -1$ is negative, while the other two are complex-valued. Note that along diag the vector field points in the diagonal direction. Moreover, the function

$(\alpha/(1+u^n)) - u$ is positive at $u = 0$, negative at $u = \alpha$, and monotone. This implies that diag constitutes the global stable manifold of R.

By symmetry, the plane of remaining eigendirections of R is orthogonal to diag. To determine the type of R, it remains to study the real part of the complex eigenvalues:

$$\mathrm{Re}\lambda = \cos\left(\pm\frac{\pi}{3}\right)\cdot\frac{nr^n}{1+r^n} - 1 = \frac{n}{2}\cdot\frac{r^n}{1+r^n} - 1.$$

As r varies from 0 to ∞ this quantity changes monotonically between -1 and $(n/2)-1$, and therefore it is always negative when $n \le 2$. However, for $n > 2$ the value

$$r_0 = \sqrt[n]{\frac{2}{n-2}} \tag{6}$$

is such that $\mathrm{Re}\lambda$ is negative for $r < r_0$ and positive for $r > r_0$. In particular, for the unique parameter

$$\alpha_{\mathrm{bif}} = r_0^{n+1} + r_0$$

(depending on n), the linearization of (1) at R has one real and two purely imaginary eigenvalues. This is the setting for a Hopf bifurcation. In an appendix we compute the first Lyapunov coefficient $\ell_1(R)$ of (1) near R, and find that $\ell_1(R) = -(n^2+5n-14)/18\sqrt{3}r_0^2$. The polynomial $-(n^2+5n-14) = -(n+7)(n-2)$ is negative for all $n > 2$. This shows that the bifurcation is supercritical; as a consequence, the cycles are attracting, and appear when $\alpha > \alpha_{\mathrm{bif}}$.

3. Orbit Dynamics

3.1. *The attracting cube $\mathcal{C}$*

In this section we prove Lemma 1; then we decompose $\mathcal{C}$ into pieces where orbit behavior is simple to describe. The proof of Lemma 1 is a consequence of the following two claims.

Claim 1. *If $0 \le x(0) \le \alpha$, then $0 < x(t) < \alpha$ for all $t > 0$.*

Claim 2. *If $x(0) \ge \alpha$, then there is a time t_1 such that $x(t_1) < \alpha$.*

Indeed, by the symmetry of the system, y and z satisfy analogous inequalities, so Claims 1 and 2 imply

(1) The cube $\mathcal{C}$ is a trapping region; i.e. the vector field is transversal to $\partial\mathcal{C}$, pointing to the interior.
(2) The orbit of any point $P \notin \mathcal{C}$ moves toward, and eventually enters $\mathcal{C}$.

These two assertions are equivalent to the statement of Lemma 1. Now, the proof of Claim 1 is immediate:

(i) If $x(0) = 0$, then $(\mathrm{d}x/\mathrm{d}t)(0) = \alpha/(1+y_0^n) > 0$.
(ii) If $x(0) = \alpha$, then $(\mathrm{d}x/\mathrm{d}t)(0) = \alpha/(1+y_0^n) - \alpha = \alpha((1/(1+y_0^n)) - 1) < 0$.

Proof of Claim 2. Generalizing the above inequality, it is obvious that $\mathrm{d}x/\mathrm{d}t < 0$ when $x \ge \alpha$. However, this is not enough to conclude Claim 2. Instead, we need to show that $\mathrm{d}x/\mathrm{d}t$ is *bounded away* from 0, and this requires the chain of estimates (7)–(10) on x, y, z, and back to x. Suppose then for a contradiction that

$$x(t) = \alpha + \varepsilon_t \ge \alpha \quad \text{for all } t \ge 0. \tag{7}$$

Notice that (7) implies $\mathrm{d}z/\mathrm{d}t \le (\alpha/(1+\alpha^n)) - z$ for all t. As long as $z(t)$ remains larger than α, the derivative $\mathrm{d}z/\mathrm{d}t \le \alpha((1/(1+\alpha^n)) - 1) < 0$ is bounded away from 0, so z decreases at a steady rate. It follows that there is a time $t_0 > 0$ such that

$$z(t) < \alpha \quad \text{for all } t > t_0. \tag{8}$$

Definition 2. The quantity $\alpha/(1+\alpha^n)$ appears frequently enough in estimates that it will be convenient to represent it with the letter A.

By Claim 1, $y(t_0) > 0$. Now, if $y(t_0) \le A$, inequality (8) gives $\mathrm{d}y/\mathrm{d}t \ge A - y > 0$ for $t > t_0$, so the y coordinate cannot become less than $y(t_0)$. On the other hand, if $y(t_0) > A$, the y coordinate cannot become A since $(\mathrm{d}y/\mathrm{d}t)|_{t_0} \ge A - y > 0$. In either case, if $Y = \min\{y(t_0), A\}$ (a positive quantity), then

$$y(t) \ge Y > 0 \quad \text{for } t > t_0. \tag{9}$$

Using (7) and (9), we find that $\mathrm{d}x/\mathrm{d}t$ is bounded away from 0:

$$\begin{aligned}\frac{\mathrm{d}x}{\mathrm{d}t} &= \alpha\left(\frac{1}{1+y^n} - 1\right) - \varepsilon_t \\ &\le \alpha\left(\frac{1}{1+Y^n} - 1\right) - \varepsilon_t < 0,\end{aligned} \tag{10}$$

so x becomes arbitrarily small, contradicting (7). This proves Claim 2 and the Lemma. ■

3.2. *Nullcline description*

We have just seen that any interesting dynamical behavior is bound to happen in $\mathcal{C}$. For the rest of the paper, x, y, z are restricted to $\mathcal{C}$. As usual, the shape and relative position of the nullcline surfaces

for the three variables is an important indicator of how the system behaves. In this section we describe the configuration of nullclines.

Definition 3. The nullclines N_x, N_y, N_z are the loci of points where each of the derivatives $\mathrm{d}x/\mathrm{d}t, \mathrm{d}y/\mathrm{d}t, \mathrm{d}z/\mathrm{d}t$ vanish. They are three surfaces given implicitly by

$$N_x = \left\{ \frac{\alpha}{1+y^n} = x \right\} \cup \mathcal{C},$$
$$N_y = \left\{ \frac{\alpha}{1+z^n} = y \right\} \cup \mathcal{C}, \tag{11}$$
$$N_z = \left\{ \frac{\alpha}{1+x^n} = z \right\} \cup \mathcal{C}.$$

Let η be the curve $\{(\alpha/(1+y^n)) - x, z = 0\}$, which connects $(\alpha, 0, 0)$ with $(A, \alpha, 0)$. Then, N_x is formed by translating η along the z-direction. The nullclines N_y and N_z are formed in a similar fashion and their union has rotational symmetry about the diagonal; see Fig. 1.

Note that N_x divides $\mathcal{C}$ in exactly two pieces, one where $\mathrm{d}x/\mathrm{d}t < 0$ and one where $\mathrm{d}x/\mathrm{d}t > 0$. Since $(\alpha/(1+y^n))' = -n\alpha y^{n-1}/(1+y^n)^2 < 0$, the curve η is monotonically decreasing in the x-direction.

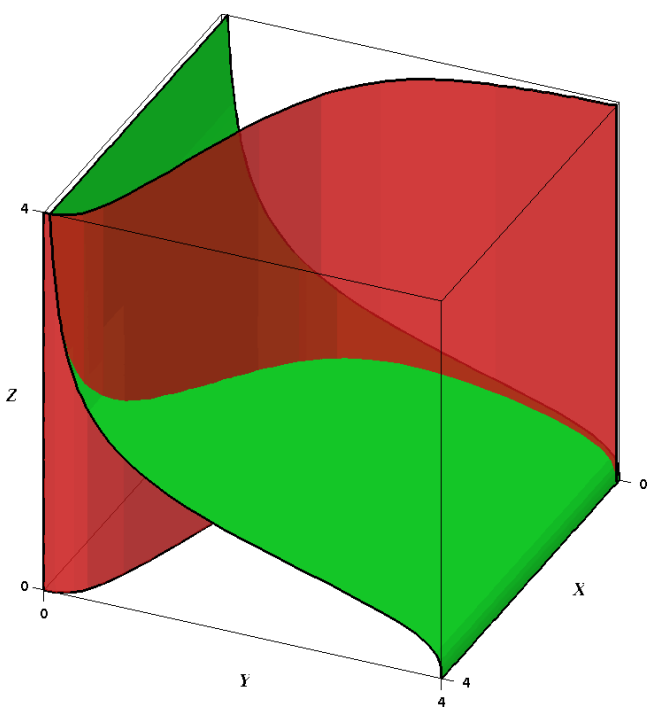

Fig. 1. ($\alpha = 4$, $n = 3$). The nullclines N_x and N_y intersect monotonically along an open-ended curve. One of the straight sides of each nullcline ends at an edge of $\mathcal{C}$, while the opposite side intersects $\mathcal{C}$ on a face, very close to the opposite edge.

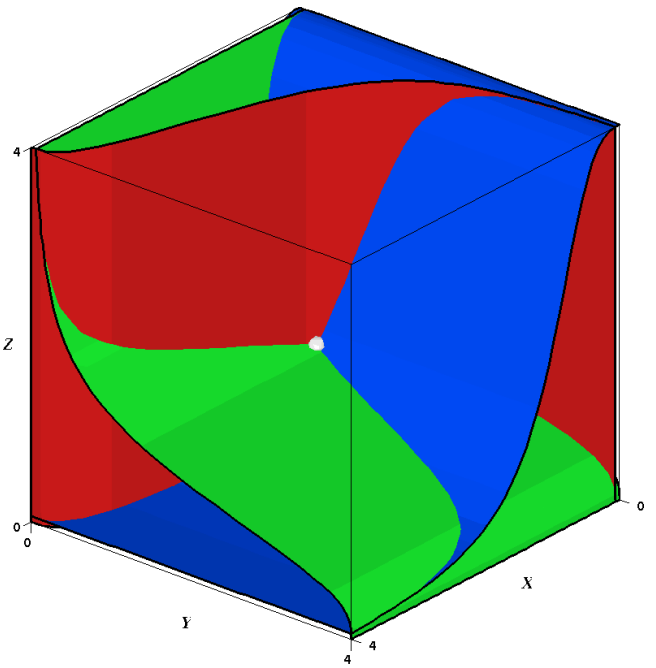

Fig. 2. ($\alpha = 4$, $n = 3$). The intersection of the three nullclines is a single point R. Their union is rotationally symmetric about the main diagonal, and divides $\mathcal{C}$ into eight regions.

The intersection of N_x with N_y is a curve β_{xy} with parametric equations

$$x(t) = \frac{\alpha}{1 + \left(\dfrac{\alpha}{1+t^n}\right)^n},$$
$$y(t) = \frac{\alpha}{1+t^n},$$
$$z(t) = t,$$

with $0 \le t \le \alpha$. This curve joins the points $(A, \alpha, 0)$ and $(\alpha/(1+A^n), A, \alpha)$. Similar descriptions hold for the nullcline intersection curves β_{yz}, β_{zx}. These three curves intersect at the single point R. It follows that the union $N_x \cup N_y \cup N_z$ divides $\mathcal{C}$ in eight regions in a manner qualitatively similar to the union of three orthogonal planes. Extending this analogy, we refer to the eight components of $\operatorname{int}\mathcal{C}\backslash(N_x \cup N_y \cup N_z)$ as *octant regions*; see Fig. 2.

3.3. *Breaking $\mathcal{C}$ into pieces*

In this section we partition $\mathcal{C}$ in several pieces where the behavior of system (1) is easy to describe. Then, we use this decomposition to prove Theorem 1.

Definition 4. The *signature* of a point $P \in \mathcal{C}$ is a triple of symbols from the alphabet $\{-, +, \mathsf{o}\}$

which describe the signs of the derivatives of x, y and z at P. We extend this notation to refer to any subset of $\mathcal{C}$ where the signs remain constant. Thus, for instance, $(+++)$ represents the octant region near the origin where $\mathrm{d}x/\mathrm{d}t, \mathrm{d}y/\mathrm{d}t, \mathrm{d}z/\mathrm{d}t > 0$, so $\mathsf{diag} \subset (+++) \cup (\circ\,\circ\,\circ) \cup (---)$. We extend this notation further, including the symbol $*$ to represent an undefined sign. For example, $N_x = (\circ * *)$.

Definition 5. The six octant regions $(++-)$, $(+-+)$, $(+--)$, $(-++)$, $(-+-)$, $(--+)$, which are disjoint from diag, are called *lateral regions*.

3.4. *The spindle $\mathcal{S}$*

In this section we construct a small neighborhood $\mathcal{S}$ of R that blends well with the orbits and with the layout of the nullclines N_* of system (1). First, we give an analogous construction in the linearization domain, and then pull it back by homeomorphism.

The nullclines of the linear system (4) are the planes

$$\{u = Qv\}, \quad \{v = Qw\}, \quad \{w = Qu\}, \qquad (12)$$

where $Q = -nr^n/(1 + r^n)$. As with system (1), these planes determine eight regions with different sign patterns for the derivatives $\mathrm{d}u/\mathrm{d}t, \mathrm{d}v/\mathrm{d}t, \mathrm{d}w/\mathrm{d}t$. We adopt the alphabet $\{+, -, \circ, *\}$.

The stable direction is along the diagonal $\{u = v = w\}$, which is contained in the regions $(+++)$ and $(---)$. The unstable manifold is the plane $\Pi = \{u + v + w = 0\}$, orthogonal to the diagonal. This plane sits inside the union of the six lateral regions.

For any $\varepsilon > 0$, consider the infinite cylinder of radius ε in the direction of the diagonal $\{u = v = w\}$. Let $m > 0$ be a fixed number (for all ε) large enough that the planes Π_+, Π_-, at distance $m\varepsilon$ from Π intersect the cylinder in two disks D_+, D_- that are completely contained in $(+++), (---)$, respectively. Denote by C_ε the compact portion of the cylinder bounded between D_+ and D_-.

The behavior of the orbit γ of any point $P \in C_\varepsilon \backslash \Pi$ is as follows. In negative time, γ spirals toward the diagonal, while monotonically moving away from Π, so that it exits C_ε in finite time through either D_+ or D_-.

In positive time, γ approaches Π monotonically while spiraling away from the diagonal (since the complex eigenvalues have positive real part). Thus, γ stays between Π_+ and Π_-. We claim that γ escapes into a lateral region at a distance d_ε from diag, where δ_ε becomes arbitrarily small as ε goes to 0. Indeed, the planes Π_+, Π_- intersect the nullcline planes in two triangles Δ_+, Δ_- contained within distance d_ε from the diagonal. The rectangular faces of the prism between Δ_+ and Δ_- are contained inside the lateral regions. Since the orbit γ intersects one of these prism faces in positive finite time, the claim follows.

Now consider the ball B_ε of radius ε centered at the origin. For any $P \in B_\varepsilon \backslash \Pi$, let s_P be the segment of the full orbit γ_P that starts in $D_+ \cup D_-$, and ends at the first point that is both inside a lateral region and outside C_ε.

Definition 6. The *linear spindle* of size ε is the union

$$S_\varepsilon = B_\varepsilon \cup \bigcup_{P \in B_\varepsilon \backslash \Pi} s_P.$$

It is a compact set such that

(a) S_ε contains B_ε and is simply connected.
(b) The intersection $S_\varepsilon \cap D_\pm$ is compactly contained in $(+++) \cup (---)$.

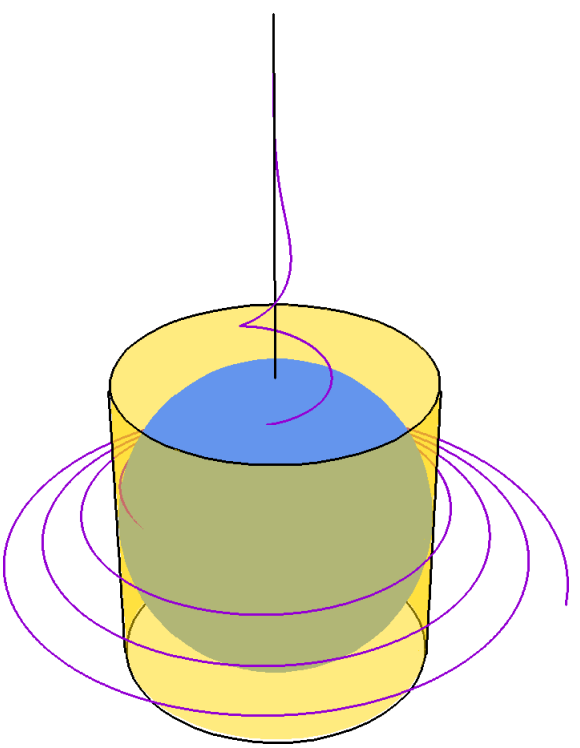

Fig. 3. The ball B_ε around the origin is encased in the cylinder C_ε. The disks $D_\pm$ at both ends of C_ε are inside the region $(+++)$ or $(---)$, so backward orbits from B_ε exit C_ε into one of these regions. The forward orbit approaches the plane Π through the equator of B_ε, so it eventually enters a lateral region. The linear spindle S_ε consists of B_ε and all the orbits that start at $D_\pm$, enter B_ε, and exit C_ε into a lateral region.

(c) Any orbit that enters S_ε does so through $S_\varepsilon \cap D_\pm$.
(d) All orbits in $S_\varepsilon \backslash \mathsf{diag}$ leave S_ε through a lateral region, never to return to S_ε (nor, in fact, to $(+++) \cup (---)$).
(e) $\lim_{\varepsilon \to 0} \operatorname{diam} S_\varepsilon = 0$.

Since the linearization of R is a saddle, there is a radius $\delta > 0$, and a homeomorphism

$$\phi : B_\delta(R) \to N$$

that conjugates the nonlinear system (1) within the ball $B_\delta(R)$, to the linearization (4) in a neighborhood N of 0. Let $\varepsilon > 0$ be small enough that the linear spindle S_ε is compactly contained in N.

Definition 7. The preimage $\mathcal{S} = \phi^{-1}(S_\varepsilon) \subset B_\delta$ will be called the *spindle* of (1). Note that ϕ takes local nullclines $N_* \cap B_\varepsilon(R)$ to the planes (12) inside N. By a slight abuse of notation, we denote by $D_\pm$ the preimages $\phi^{-1}(D_\pm)$ in $(+++), (---) \subset \mathcal{C}$. With these considerations in mind, $\mathcal{S}$ satisfies

(a) $\mathcal{S}$ is simply connected.
(b) The intersection $\mathcal{S} \cap D_\pm$ is compactly contained in $(+++) \cup (---)$.
(c) Any orbit that enters $\mathcal{S}$ does so through $\mathcal{S} \cap D_\pm$.
(d) All orbits in $\mathcal{S} \backslash \mathsf{diag}$ leave $\mathcal{S}$ through a lateral region and escape B_δ without re-entering $\mathcal{S}$.

In particular, if an orbit that leaves $\mathcal{S}$ were to return to $\mathcal{S}$, it would have to follow a homoclinic connection. One consequence of Proposition 3 below will be that this does not happen.

3.5. *The trapping torus T*

Definition 8. The region $T = \mathrm{cl}(--+) \cup \mathrm{cl}(-+-) \cup \mathrm{cl}(-++) \cup \mathrm{cl}(+--) \cup \mathrm{cl}(+-+) \cup \mathrm{cl}(++-) \backslash \operatorname{int} \mathcal{S}$ (where cl stands for closure) has the topological type of a filled torus. It is divided into six pieces whose interiors are just lateral octant regions truncated by $\mathcal{S}$. We call these truncated regions *torus pieces.*

4. Poincaré Map

Our first lemma discusses the way in which the vector fields cross the nullclines.

Lemma 2. *The orbit of $P \in N_x \backslash R$ moves into an octant region according to the following table.*

$P \in (\mathsf{o}++)$	moves inside$(-++)$
$(\mathsf{o}+-)$	$(-+-)$
$(\mathsf{o}-+)$	$(+-+)$
$(\mathsf{o}--)$	$(+--)$
$(\mathsf{o}\,\mathsf{o}+)$	$-\,''\,-\,(+-+)$
$(\mathsf{o}\,\mathsf{o}-)$	$(-+-)$
$(\mathsf{o}+\mathsf{o})$	$(-++)$
$(\mathsf{o}-\mathsf{o})$	$(+--)$

The behavior for a point P in N_y or N_z is analogous, and the corresponding table is obtained from the above one by permuting the coordinates.

Proof. Since the tangent plane of N_x at any point contains the vector $\langle 0, 0, 1 \rangle$, the vector field is parallel to N_x exactly on the intersection $N_x \cap N_y = (\mathsf{o}\,\mathsf{o}*)$. Let $\mathbf{n}$ be a normal vector to N_x at P pointing away from the z-axis. Recall that $f(u) = \alpha/(1+u^n)$ has negative derivative. Then $\mathbf{n}$ is of the form $\langle 1, -f'(y), 0 \rangle$. If $P \in (\mathsf{o}+*)$, the dot product of $\mathbf{n}$ with a flow vector of the form $(\mathsf{o}+*)$ must be positive, while if $P \in (\mathsf{o}-*)$, the dot product is negative.

Orbit behavior for points on the other two nullclines can be deduced from this table by permuting the three coordinates. ■

Next we show that orbits must cross between octant regions.

Definition 9. A point $P \in \mathcal{C} \backslash R$ is *close to* diag if its forward orbit enters $\mathcal{S}$.

Proposition 2. *Let $P = P(0) \in \mathcal{C} \backslash \mathsf{diag}$ lie in the interior of any octant region. Then the orbit of P will cross in finite time to a different lateral region and outside the spindle.*

Proof. If P is close to diag, its orbit enters $\mathcal{S}$ in finite time by the construction of $\mathcal{S}$. Then, since it is not in diag, it crosses over to a lateral region. This proves the claim in this case.

Now assume that P is in a given octant region, but not close to diag. By definition the forward orbit does not enter $\mathcal{S}$, so there is an ε such that for all $t > 0$, $P(t)$ is at least ε-away from R. Since R is the only point with vanishing derivative, there is a $\delta > 0$ such that $||P'(t)|| > \delta$ for all $t > 0$. Thus, at any given time t one of the three coordinates has speed larger than δ. After $t > 3\alpha/\delta$, one of the three variables had speed larger than δ for a union of disjoint time

intervals of total length at least α/δ. Assuming that the orbit remains in the same octant region for all time, this coordinate changes monotonically. By the Mean Value Theorem it follows that this coordinate changes by at least α, hence P would escape $\mathcal{C}$.

This contradiction proves that the orbit of P must cross through a nullcline to a different octant region. This new region cannot be $(+++)$ or $(---)$ because of the transition pattern from Lemma 2. ■

We continue by showing that the torus T is a trapping region, and we describe the behavior of the flow inside T.

Proposition 3. *The following hold*

(1) *All orbits in* $\mathcal{C}\backslash\mathsf{diag}$ *are trapped in finite time in the interior of* T.
(2) *Inside* T *every orbit moves from torus piece to torus piece, crossing nullclines in the following pattern*:

$$\begin{aligned}(\mathsf{o}-+) &\mapsto (+-+) \mapsto (+-\mathsf{o}) \mapsto (+--)\\ &\mapsto (+\mathsf{o}-) \mapsto (++-) \mapsto (\mathsf{o}+-)\\ &\mapsto (-+-) \mapsto (-+\mathsf{o}) \mapsto (-++)\\ &\mapsto (-\mathsf{o}+) \mapsto (--+) \mapsto (\mathsf{o}-+).\end{aligned} \tag{13}$$

Proof. Let $P \in \mathcal{C}\backslash\mathsf{diag}$. If $P \in \partial\mathcal{C}$, by Lemma 1 the flow points toward the interior of T. By Proposition 2, if P is in an octant region, its forward orbit enters $\operatorname{int} T$ in finite time. If P is anywhere on a nullcline, then Lemma 2 and the construction of the spindle prove the first claim.

Each torus piece is bounded by five surfaces; a portion of $\partial\mathcal{C}$, a portion of $\partial\mathcal{S}$, and three nullcline components (one from each of N_x, N_y, N_z). Let us call the latter three *faces* of the torus piece.

Now consider a torus piece, say $(+-+)$. Its three faces are truncations of $(\mathsf{o}-+)$, $(+\mathsf{o}+)$ and $(+-\mathsf{o})$. Again, by Lemma 2, the flow enters $(+-+)$ through the first two faces, and exits L toward $(+--)$ only through the third face. The same argument applied to the remaining five torus pieces proves that the only possible transitions between torus pieces are given by the pattern (13). ■

Definition 10. Denote by $K_x = \operatorname{cl}(\mathsf{o}-+) \cap T$.

Corollary 1. *There is a well defined Poincaré return map*

$$\theta : K_x \to K_x.$$

The proof is immediate from Proposition 3.

Theorem 1 follows from Brower's Fixed point Theorem applied to the map θ. Moreover, any such cycle must move through lateral regions in the pattern (13).

Acknowledgments

The second author was supported by NSF grant DMS-0817717 and International Development Grant of Indiana University. The third author was supported by NSF grant DMS-0701557.

References

Atkinson, M., Savageau, M., Myers, J. & Ninfa, A. [2003] "Development of genetic circuitry exhibiting toggle switch or oscillatory behavior in escherichia coli," *Cell* **113**, 597–607.

Barkai, N. & Leibler, S. [2000] "Circadian clocks limited by noise," *Nature* **403**, 267–268.

Buşe, O., Kuznetsov, A. & Pérez, R. A. [2009] "Dynamical properties of the repressilator model," submitted to *Phys. Rev. E.*

Devaney, R., Hirsh, M. & Smale, S. [2004] *Differential Equations, Dynamical Systems, and an Introduction to Chaos* (Elsevier/Academic Press).

Dunlap, J. C. [1999] "Molecular bases for circadian clocks," *Cell* **96**, 271–290.

Elowitz, M. & Leiber, S. [2000] "A synthetic oscillatory network of transcriptional regulators," *Nature* **403**, 335–338.

Hasty, J., Isaacs, F., Dolnik, M., McMillen, D. & Collins, J. J. [2001] "Designer gene networks: Towards fundamental cellular control," *Chaos* **11**, 207–220.

Kuznetsov, A., Kaern, M. & Kopell, N. [2004] "Synchrony in a population of hysteresis-based genetic oscillators," *SIAM J. Appl. Math.* **65**, 392–425.

Kuznetsov, Y. [2004] *Elements of Applied Bifurcation Theory*, Applied Mathematical Sciences, Vol. 112 (Springer).

Munkres, J. R. [2000] *Topology: A First Course*, 2nd edition (Prentice-Hall).

Nurse, P. [2000] "A long twentieth century of the cell cycle and beyond," *Cell* **100**, 71–78.

Yang, D., Li, Y. & Kuznetsov, A. [2009] "Characterization and merger of oscillatory mechanisms in an artificial genetic regulatory network," submitted to *Chaos.*

Appendix

Here, we compute the first Lyapunov coefficient $\ell_1(R)$ of system (1) near R when $\alpha = \alpha_{\text{bif}}$. Recall that the bifurcation condition is expressed by

$$r = r_0 = \sqrt[n]{\frac{2}{n-2}}.$$

Let us first rewrite the vector field in the format

$$F(x,y,z) = (f(x,y,z), g(x,y,z), h(x,y,z)) = \left(\frac{\alpha}{1+y^n} - x, \frac{\alpha}{1+z^n} - y, \frac{\alpha}{1+x^n} - z\right).$$

The third order Taylor approximation of F around R has a particularly simple expression because only partial derivatives of higher order that do not vanish are $f_{y\cdots y}$, $g_{z\cdots z}$, and $h_{x\cdots x}$ (compare (3)). Indeed,

$$F(x,y,z) = A\cdot\begin{pmatrix}x\\y\\z\end{pmatrix} + \frac{1}{2!}B((x,y,z),(x,y,z)) + \frac{1}{3!}C((x,y,z),(x,y,z),(x,y,z)) + O(|(x,y,z)|^4),$$

where A is the jacobian matrix

$$\begin{pmatrix} -1 & \dfrac{-nr_0^n}{1+r_0^n} & 0 \\ 0 & -1 & \dfrac{-nr_0^n}{1+r_0^n} \\ \dfrac{-nr_0^n}{1+r_0^n} & 0 & -1 \end{pmatrix} = \begin{pmatrix} -1 & -2 & 0 \\ 0 & -1 & 2 \\ -2 & 0 & -1 \end{pmatrix}$$

with eigenvalues $-3, \pm\sqrt{3}i$ (regardless of n), and B and C are bi- and trilinear functions respectively, with components

$$B_1((x_1,y_1,z_1),(x_2,y_2,z_2)) = f_{yy|_{x,y,z=r_0}}\cdot y_1y_2,$$
$$B_2((x_1,y_1,z_1),(x_2,y_2,z_2)) = g_{zz|_{x,y,z=r_0}}\cdot z_1z_2,$$
$$B_3((x_1,y_1,z_1),(x_2,y_2,z_2)) = h_{xx|_{x,y,z=r_0}}\cdot x_1x_2,$$

and

$$C_1((x_1,y_1,z_1),(x_2,y_2,z_2),(x_2,y_2,z_2)) = f_{yyy|_{x,y,z=r_0}}\cdot y_1y_2y_3,$$
$$C_2((x_1,y_1,z_1),(x_2,y_2,z_2),(x_2,y_2,z_2)) = g_{zzz|_{x,y,z=r_0}}\cdot z_1z_2z_3,$$
$$C_3((x_1,y_1,z_1),(x_2,y_2,z_2),(x_2,y_2,z_2)) = h_{xxx|_{x,y,z=r_0}}\cdot x_1x_2x_3.$$

The following formula applies in the general setting of a Hopf bifurcation.

Lemma 3 [Kuznetsov, 2004, p. 180]. *Let* $\mathbf{q}$ *be the eigenvector of* A *corresponding to the eigenvalue* $\sqrt{3}i$*, normalized so that* $\overline{\mathbf{q}}\cdot\mathbf{q} = 1$*. Let* $\mathbf{p}$ *be the adjoint eigenvector such that* $A^{\mathrm{T}}\mathbf{p} = -\sqrt{3}i\mathbf{p}$ *and* $\overline{\mathbf{p}}\cdot\mathbf{q} = 1$*. If* I *denotes the* 3×3 *unit matrix, then*

$$\ell_1(R) = \frac{1}{2\sqrt{3}}\mathrm{Re}(\overline{\mathbf{p}}\cdot C(\mathbf{q},\mathbf{q},\overline{\mathbf{q}}) - 2\overline{\mathbf{p}}\cdot B(\mathbf{q}, A^{-1}B(\mathbf{q},\overline{\mathbf{q}})) + \overline{\mathbf{p}}\cdot B(\overline{\mathbf{q}}, (2\sqrt{3}iI - A)^{-1}B(\mathbf{q},\mathbf{q}))). \quad \text{(A.1)}$$

We will proceed as follows. First, we write explicit expressions for B and C; then we find $\mathbf{q}$ and $\mathbf{p}$. Finally, we compute the expressions in formula (A.1).

Note that $f_y(x,y,z) = -n\alpha y^{n-1}/(1+y^n)^2$, so

$$f_{yy}(x,y,z) = n\alpha\frac{(n+1)y^{2n-2} - (n-1)y^{n-2}}{(1+y^n)^3}. \quad \text{(A.2)}$$

Substituting $y = r_0$, and recalling that $\alpha/(1+r_0^n) = r_0$, we find that the coefficient of B_1 is

$$n\frac{(n+1)r_0^{2n-1} - (n-1)r_0^{n-1}}{(1+r_0^n)^2} = \frac{n}{r_0}\cdot\frac{(n+1)\left(\frac{2}{n-2}\right)^2 - (n-1)\left(\frac{2}{n-2}\right)}{\left(\frac{n}{n-2}\right)^2}$$
$$= \frac{2}{r_0}\cdot\frac{2(n+1) - (n-2)(n-1)}{n}$$
$$= \frac{2}{r_0}(5-n).$$

By symmetry, this is also the coefficient of B_2 and B_3, so the bilinear function B is

$$B((x_1,y_1,z_1),(x_2,y_2,z_2)) = \frac{2}{r_0}(5-n)(y_1y_2, z_1z_2, x_1x_2).$$

We find C in the same manner. From (A.2),

$$f_{yyy}(x,y,z) = -n\alpha\frac{(n^2+3n+2)y^{3n-3} - (4n^2-4)y^{2n-3} + (n^2-3n+2)y^{n-3}}{(1+y^n)^4}.$$

Substituting $y = r_0$ and $\alpha/(1+r_0^n) = r_0$, the coefficient of C_1 becomes

$$\begin{aligned}
&n\frac{-(n^2+3n+2)r_0^{3n-2} + (4n^2-4)r_0^{2n-2} - (n^2-3n+2)r_0^{n-2}}{(1+r_0^n)^3}\\
&\quad= \frac{n}{r_0^2}\cdot\frac{-(n^2+3n+2)\left(\frac{2}{n-2}\right)^3 + (4n^2-4)\left(\frac{2}{n-2}\right)^2 - (n^2-3n+2)\left(\frac{2}{n-2}\right)}{\left(\frac{n}{n-2}\right)^3}\\
&\quad= \frac{2}{r_0^2}\cdot\frac{-4(n+1)(n+2) + 8(n-2)(n-1)(n+1) - (n-2)^3(n-1)}{n^2}\\
&\quad= \frac{2}{r_0^2}(-n^2+15n-38),
\end{aligned}$$

and the trilinear function C becomes

$$\begin{aligned}
&C((x_1,y_1,z_1),(x_2,y_2,z_2),(x_3,y_3,z_3))\\
&\quad= \frac{2}{r_0^2}(-n^2+15n-38)(x_1x_2x_3, y_1y_2y_3, z_1z_2z_3).
\end{aligned}$$

Let $\omega = (-1/2) + (\sqrt{3}i/2)$ be a cubic root unity. Then the normalized eigenvectors $\mathbf{q}$ and $\mathbf{p}$ of Lemma 3 are

$$\mathbf{q} = \mathbf{p} = \left\langle\frac{\omega^2}{\sqrt{3}}, \frac{\omega}{\sqrt{3}}, \frac{1}{\sqrt{3}}\right\rangle. \tag{A.3}$$

Note that formula (A.1) has nested instances of the bilinear form B. These values are

$$B(\mathbf{q},\mathbf{q}) = \frac{2(5-n)}{3r_0}\langle\omega^2,\omega,\omega\rangle,$$

and

$$B(\mathbf{q},\overline{\mathbf{q}}) = \frac{2(5-n)}{3r_0}\langle 1,1,1\rangle.$$

For the outer expressions involving B we find the inverse matrices

$$A^{-1} = \begin{pmatrix} \frac{-1}{9} & \frac{2}{9} & \frac{-4}{9}\\ \frac{-4}{9} & \frac{-1}{9} & \frac{2}{9}\\ \frac{2}{9} & \frac{-4}{9} & \frac{-1}{9}\end{pmatrix},$$

$$(2\sqrt{3}iI - A)^{-1} = \begin{pmatrix} \frac{3}{63} - \frac{34\sqrt{3}i}{189} & \frac{10}{63} + \frac{8\sqrt{3}i}{189} & \frac{-4}{63} + \frac{8\sqrt{3}i}{189}\\ \frac{-4}{63} + \frac{8\sqrt{3}i}{189} & \frac{3}{63} - \frac{34\sqrt{3}i}{189} & \frac{10}{63} + \frac{8\sqrt{3}i}{189}\\ \frac{10}{63} + \frac{8\sqrt{3}i}{189} & \frac{-4}{63} + \frac{8\sqrt{3}i}{189} & \frac{3}{63} - \frac{34\sqrt{3}i}{189}\end{pmatrix},$$

so that

$$A^{-1}B(\mathbf{q},\overline{\mathbf{q}}) = \frac{-2(5-n)}{9r_0^2}\langle 1,1,1\rangle,$$

$$\begin{aligned}
&(2\sqrt{3}iI - A)^{-1}B(\mathbf{q},\mathbf{q})\\
&\quad= \frac{-(5-n)}{27r_0}\left\langle 1 - \frac{i}{\sqrt{3}}, \frac{6-4\sqrt{3}i}{7}, -3-\sqrt{3}i\right\rangle.
\end{aligned}$$

Then

$$B(\mathbf{q}, A^{-1}B(\mathbf{q},\overline{\mathbf{q}})) = \frac{-4\sqrt{3}(5-n)^2}{27r_0^2}\langle\omega,1,\omega^2\rangle,$$

and

$$\begin{aligned}
&B(\overline{\mathbf{q}}, (2\sqrt{3}iI - A)^{-1}B(\mathbf{q},\mathbf{q}))\\
&\quad= \frac{-2\sqrt{3}(5-n)^2}{27r_0^2}\left\langle 1 - \frac{i}{\sqrt{3}}, -1 - \frac{i}{\sqrt{3}}, \frac{2}{\sqrt{3}}i\right\rangle.
\end{aligned}$$

The last function value needed is

$$C(\mathbf{q},\mathbf{q},\overline{\mathbf{q}}) = \frac{\sqrt{3}(n^2-15n+38)}{9r_0^2}\langle 1-\sqrt{3}i, -2, \sqrt{3}-3i\rangle.$$

Now we can compute the hermitian products

$$\overline{\mathbf{p}} \cdot C(\mathbf{q}, \mathbf{q}, \overline{\mathbf{q}}) = \frac{n^2 - 15n + 38}{3r_0^2}(1 + \sqrt{3}i), \tag{A.4}$$

$$\overline{\mathbf{p}} \cdot B(\mathbf{q}, A^{-1}B(\mathbf{q}, \overline{\mathbf{q}})) = \frac{2(5-n)^2}{9r_0^2}(1 + \sqrt{3}i), \tag{A.5}$$

and

$$\overline{\mathbf{p}} \cdot B(\overline{\mathbf{q}}, (2\sqrt{3}iI - A)^{-1}B(\mathbf{q}, \mathbf{q})) = \frac{4(5-n)^2}{9\sqrt{3}r_0^2}i. \tag{A.6}$$

Putting together (A.4)–(A.6), the Lyapunov coefficient is

$$\begin{aligned} \ell_1(R) &= \frac{-1}{18\sqrt{3}r_0^2}\mathrm{Re}(n^2 + 5n - 14 + 13\sqrt{3}n^2 i \\ &\quad - 115\sqrt{3}ni + 286\sqrt{3}i) \\ &= \frac{-(n^2 + 5n - 14)}{18\sqrt{3}r_0^2}. \end{aligned} \tag{A.7}$$